

Article

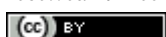
Estimating and mapping woodland biomass and carbon using Landsat 8 vegetation index: A case study in Dirmaga Watershed, Ethiopia

M. Adamsew Maregn, D. Temesgen Mekonen

Department of Natural Resource Management, College of Agriculture and Environmental Sciences, University of Gondar, P.O. Box 196, Gondar, Ethiopia

E-mail: Adamsew.Maregn@uog.edu.et, adamsewmaregn@gmail.com, temelrm2003@gmail.com

Received 19 February 2022; Accepted 11 March 2022; Published 1 June 2022



Abstract

This study was conducted to estimate the above and below ground carbon storage in the Woodlands of Dirmaga Watershed, North Western Ethiopia. The field data were collected through systematic random sampling techniques of 40 sample plots. The above-ground biomass and below-ground biomass of the study area was collected from 20 m × 20 m area of the main plot. The biomass and carbon stock of the woodland was estimated using site-specific allometric models and Landsat 8 NDVI and analyzed by ArcGIS. The result showed that the mean carbon stock of above-ground carbon and below-ground carbon were accounted for about 291.47 t/ha and 24.81 t/ha, respectively. The relationship between AGC and NDVI was strong with correlation coefficient of 0.86 and R^2 value of 0.745. Tree species of *Anogeissus leiocarpa*, *Adansonia digitata* and *Diospyros mespiliformis* sequestered the largest portion of the carbon stockwhile, *Ficus sycomorus L.*, *Rhus glutinosa* and *Securinega virosa* were the least contributor of carbon stock. The woodland has a great potential for carbon sequestration and biodiversity conservation and the concerned body should conserve and manage the resource properly.

Keywords carbon stock; woodland; allometric equation; NDVI; regression; correlation.

Computational Ecology and Software
ISSN 2220-721X
URL: <http://www.iaees.org/publications/journals/ces/online-version.asp>
RSS: <http://www.iaees.org/publications/journals/ces/rss.xml>
E-mail: ces@iaees.org
Editor-in-Chief: WenJun Zhang
Publisher: International Academy of Ecology and Environmental Sciences

1 Introduction

Forest ecosystems are major components of the earth's energy cycles and provide significant environmental services. Forest biomass is an important metric for defining the structure and function of woodlands (West, 2009; Lieth and Whittaker, 1975). Many ecosystem processes are influenced by forest biomass, and many processes are affected by forest biomass (Tian et al., 2014). Forests are the most abundant and greatest source of terrestrial carbon sinks, contributing significantly to the global carbon cycle. By implementing C sequestration in biomass and soils, they play a critical role in reducing the climate change scenario (IPCC,

2019). Because quantifying forest belowground biomass is difficult, most previous research have concentrated on forest aboveground biomass (AGB).

Estimating AGB is a necessary step in determining carbon stocks and balances (Ketterings et al., 2001). Process-based ecosystem models, field measurements, and a combination of forest inventory plots and remotely sensed data have all been used to estimate forest AGB in previous research (Lu et al., 2016; Safari et al., 2017). For numerous reasons, the remote-sensing-based technique has been popular in recent decades: (1) Remote sensing data covers large areas, allowing for the assessment of vegetation spatial variation and determining the spatial distribution and pattern of biomass in large areas and complex forest landscapes; (2) forest biomass research at various scales can be conducted using multiple sensors and spatial resolutions and (3) multi-temporal remote sensing images provide long-term, dynamic, and continuous AGB observations (Lu, 2006).

The rapid advancement of remote sensing technology has resulted in a large amount of remotely sensed images data that can be used to estimate AGB. The information can be separated into three groups: (1) Landsat, Systeme Probatoire d'Observation de la Terre (SPOT), moderate-resolution imaging spectroradiometer (MODIS), QuickBird, ASTER, Advanced Very High-Resolution Radiometer (AVHRR), and China-Brazil earth resource satellite (CBERS) are examples of optical remote sensing data; (2) active remote sensing data such as Radar and Lidar are examples of active remote sensing data; and (3) the integration of multisource remote sensing (Lu et al., 2016; Galidaki et al., 2017; Mitchard et al., 2009; Sun et al., 2011) Specifically, Because the images are free to download, have medium spatial (30 m × 30 m) and temporal (16 days) resolutions, and cover a large area, Landsat has been widely used to estimate forest biomass in conjunction with sample plots (Zhu et al., 2016; Zhu and Liu, 2015). Landsat's geographical resolution is comparable to the size of sample plots in national forest inventories in many countries, which reduces spatial errors in matching pixels and sample plots (Sun et al., 2015).

Forest stands with varying biomass typically have varied forest architecture and biophysical properties. These characteristics appear as varied hues, structures, and textures in remote sensing photographs. Using feature extraction methods, the image parameters that are closely related to forest biomass can be extracted from the remote sensing images, and forest biomass can be estimated. Vegetation information in remote sensing images is mainly reflected by the spectral characteristics.

The objectives of this study were to estimate and map the aboveground biomass and carbon of woodlands in Dirmaga Watershed through in-situ vegetation inventory and correlating with net deferece vegetation index values to map spatial above ground carbon.

2 Materials and Methods

2.1 Description of study area

Dirmaga Watershed is found in West Gondar Administrative Zone, West Armachiho District in Amhara Region. Most part of the watershed is laid on Godebie National Park. Geographically, it is located on 13°12'20.51'' to 13°25'18.4'' N latitude and 36°13'56.73'' to 36°30'0.3'' East longitudes with an altitudinal range of 625 m to 1183 m above sea level. The area is hotter throughout the year having annual temperature range of 38-48°C and the area receives 600-1100mm annual rain fall stayed from June – August (Hurni, 1998). Based on the long-term weather variable records of Global weather data records (1979-2013) calibrated with ground truth data from the nearest Abraha Jira Station, the mean annual rainfall is 780 mm with a monomodal rainfall season ranges from June to August, which contributes about 82% of the annual rainfall of the study area (<https://globalweather.tamu.edu>). The temperatures range from 15.1°C to 40°C with mean annual temperature of 27.1°C.

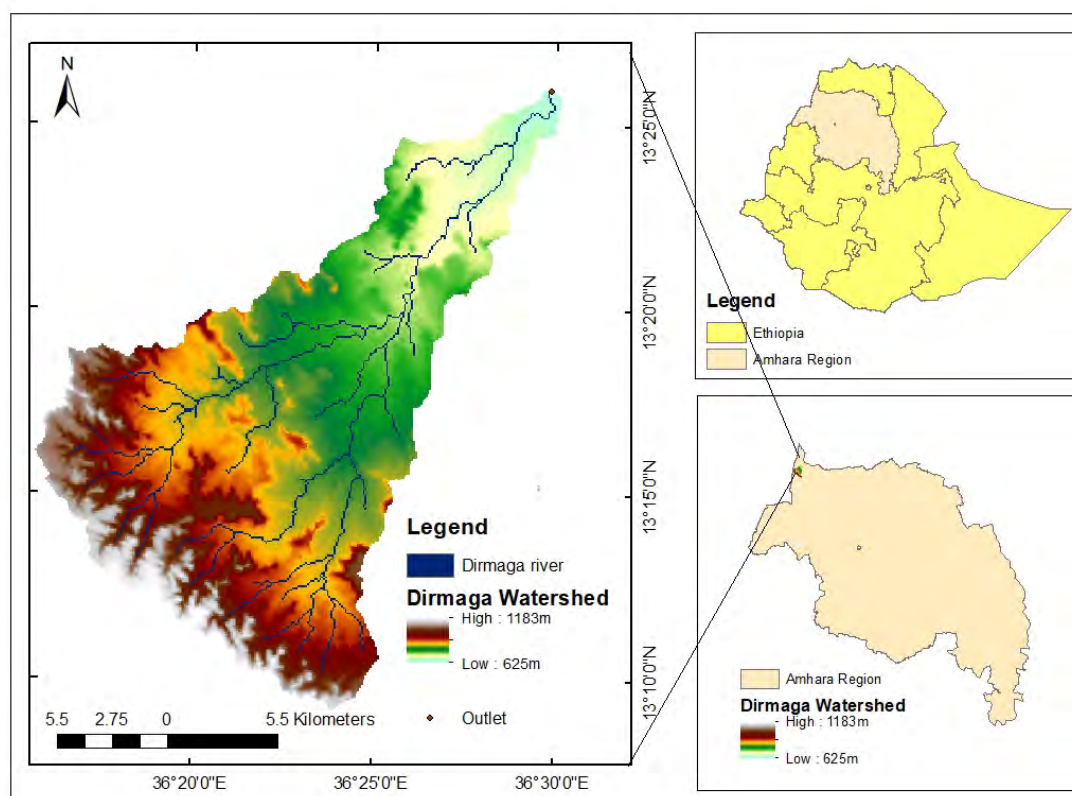


Fig. 1 Location map of the study area.

Based on vegetation classification of Ethiopia Ib Friis (2010), Godebie National Park Forest communities are broadly categorized as *Combretum-Terminalia* woodland and wooded grassland with *Terminalia brownii*, *Anogeissus leiocarpa* and *Dalbergia melanoxylon* as frequent species; *Acacia-Commiphora* woodland and bushland proper with dominant *Acacia seyal*, and *Acacia polycantha* species; and riparian/riverine forest with *Adansonia digitata*, *Diospyros mespiliformis* and *Tamarindus indica* as dominant species.

The elevation of Dirmaga watershed is ranged from 625 up to 1185 m above sea level. The major soil types of the watershed are Eutric nitisols, Chromic vertisol, and Orthic luvisols. The 55% area of Dirmaga watershed is demarcated by the district land administrative office as protected area (Part of Godebie National Park and the remaining area is pasture land and farming land. But, still now there is some illegal farming and animal husbandry on the area which has negative influence on the regeneration status of the existing vegetation.

2.2 Collection methods for vegetation inventory

2.2.1 Sampling design and sample size

The field survey was performed in the month of March 2021. Systematic sampling was employed for vegetation data collection to ensure that sufficient representative samples of vegetation from all gradient levels (Krebs, 1999; Kent, 2012). Following the procedure used in (Senbeta and Teketay, 2001; Fisaha et al., 2013; Temesgen, 2020). five transect lines were laid in the watershed following along the gradient (elevation). Based on the above principles 40 Square sample quadrats with a size of 20 m × 20 m were laid down alternatively along the line transects at 500 m intervals along the linear transects using GPS and Compass.

Carbon in the AGB (above ground biomass) was assessed through measurement of standing trees and shrubs using proper mensuration techniques. Diameter at breast height (DBH) and height (H) of trees were

measured according to their size class in the respective subplots. Therefore, species type, diameter at breast height (DBH) and height of trees (H) were the interest of measurement for trees. GPS was used to identify exact location of plots and elevation. DBH was measured with calliper/diameter tape depending on the size of the tree. Tree height was measured using haga hypsometer and graduated stick, and slope was measured with suunto clinometer to adjust the size of the plots to proper size.

2.2.2 Estimation of biomass and carbon stocks

Carbon stock has been assessed in five forest carbon pools, which is in accordance with the IPCC 2006 guideline. Hence, the major activities of carbon measurement during the field data collection were focused on above-ground biomass and below-ground biomass.

Carbon stock assessments in Africa are highly variable and have high degree of uncertainty due to lack of consistency in techniques of inventory and lack of site and species specific allometric equations. There are few species specific allometric equations developed in Africa, and most of the carbon stock assessments used general allometric equations. But this causes the high degree of variability in site growth conditions and growth characteristics of species as well as it cannot estimate the correct biomass and carbon.

Therefore, Species-specific allometric equations are very important and, in this regard, there are allometric models (Andargie et al., 2018) which are appropriate for improving aboveground biomass (AGB) and carbon (AGC) estimations in woodland ecosystems in Ethiopia and near to study area in particular. Thus, this study used the following equation developed by Andargie et al. (2018) as follows:

$$\ln(AGB) = -2.965 + 1.820 \ln(DBH) + 1.157 \ln(H) \dots \dots \dots (1)$$

where H is total height; DBH is diameter at breast height; AGB is aboveground biomass; and ln is natural logarithm. The above-ground carbon (AGC) and above-ground biomass CO₂ equivalent (AGB CO₂eq) sequestered in the study area was calculated by the principles of Pearson et al. (2005) and (2007) as follows:

$$AGC = AGB * 0.5) \dots \dots \dots (2)$$

$$AGB \text{ CO}_2\text{eq} = AGC \times 3.67 \dots \dots \dots (3)$$

According to Mac Dicken (1997) and Pearson et al. (2005) standard methods of estimating belowground biomass (BGB) and belowground carbon (BGC) can be obtained as 20% (AGB*0.2) and 10% (AGC*0.5) of above-ground tree biomass, respectively.

2.3 Vegetation index based forest carbon stock estimation

2.3.1 Satellite data sources and acquisition

The Landsat 8 NDVI (Net difference vegetation index) for the study watershed were downloaded from climate engine (<https://app.climateengine.com/climateEngine>). The Landsat 8 NDVI data is acquired in respect to the ground sampling date. The meta data of the vegetation index (NDVI) is presented in Table 1.

Table 1 Descriptions of satellite datasets used in the study.

| Satellite Data | Landsat 8 NDVI |
|------------------------------|----------------|
| Path /horizontal tile number | 170 |
| Row/ vertical tile number | 51 |
| Spatial Resolution | 30 m |
| years | March 27, 2021 |

NDVI is considered as one of the most preferred spectral indices to differentiate vegetated regions from non-vegetated regions (Tucker, 1979). The NDVI is a term which indicates the photosynthetically active radiation for vegetation (Rani et al., 2018), that is strongly affected by climatic conditions, and surrounding factors such as soil and geomorphology as well as physio-chemical characteristics of plant and leaf texture. It transforms the image of NIR and Red channels into a single band image with values ranging between -1 and +1. The values of NDVI indicate the amount of chlorophyll content present in vegetation, where higher NDVI value indicates dense and healthy vegetation and lower value indicates sparse vegetation/bare soil. To identify and assess the relationship between NDVI of the study sites, regression analysis is employed in the study. To obtain the pixel values associated with carbon of the forest, the NDVI equation was used:

$$NDVI = \frac{NIR-Red}{NIR+Red} \dots\dots\dots(4)$$

NDVI: Normalized Difference Vegetation Index, NIR: Near Infrared Band and Red: Red Band.

2.3.2 NDVI based forest carbon estimation

To estimate the forest carbon, the NDVI values were obtained from climate engine. The exact geographic coordinates of the sampling plots were obtained with the help of GPS. Ground truth points were imported to generate vector data (point) in Arc GIS environment and the resulting vector data was overlaid on the NDVI raster to extract the NDVI values. The extracted NDVI values were regressed with the field measured forest carbon values for statistical analysis. The linear equation therefore, obtained was used to generate the final estimated carbon map of the study area.

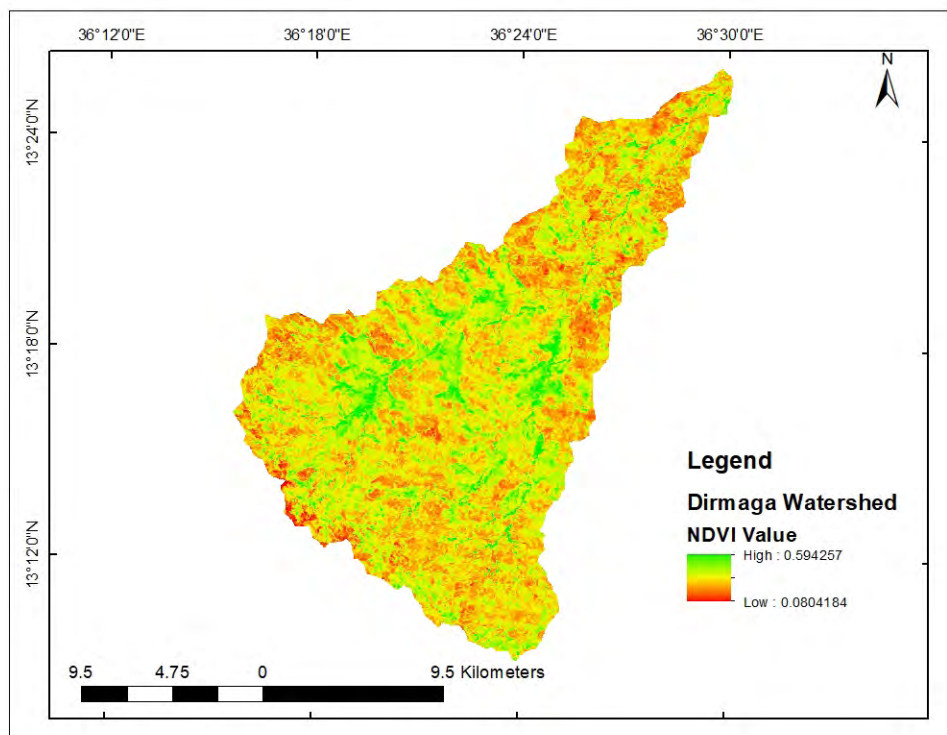


Fig. 2 Stretched NDVI value of the study area for March 27, 2021.

The linear regression model between field measured above ground carbon and NDVI generated an equation: $y = 453.46(\text{NDVI}) - 58.124$, at $p < 0.05$, where y = estimated forest carbon, 453.46 and -58.124 are regression coefficients (Table 3). The Vegetation carbon was generated from the Landsat 8 datasets. This enables to have field and satellite-derived forest carbon for comparison and validation. This also provides a comparable idea of the spatial distribution of above ground carbon over the study site.

2.4 Data analysis

SAS version 9 and Arc map 10.3 software were used as a tool to analyzed all the statistical data and spatial data respectively. Descriptive statistics was used to summarize the data, including the mean, maximum, minimum and standard deviations of carbon stock of the study area. Inferential statistics of regression and correlation analysis were used for modeling the link between forest carbon stock and NDVI.

3 Results and Discussion

3.1 Distribution of diameter at breast height (DBH) and height distribution

About 55.5% and 36.7% of the measured DBH falls between 5-10 cm diameter and between 10-29 cm diameter respectively (Fig. 3). About half percent (50%) had DBH of above 90 cm. The minimum recorded DBH was 5.0 and the maximum recorded DBH was 227 cm.

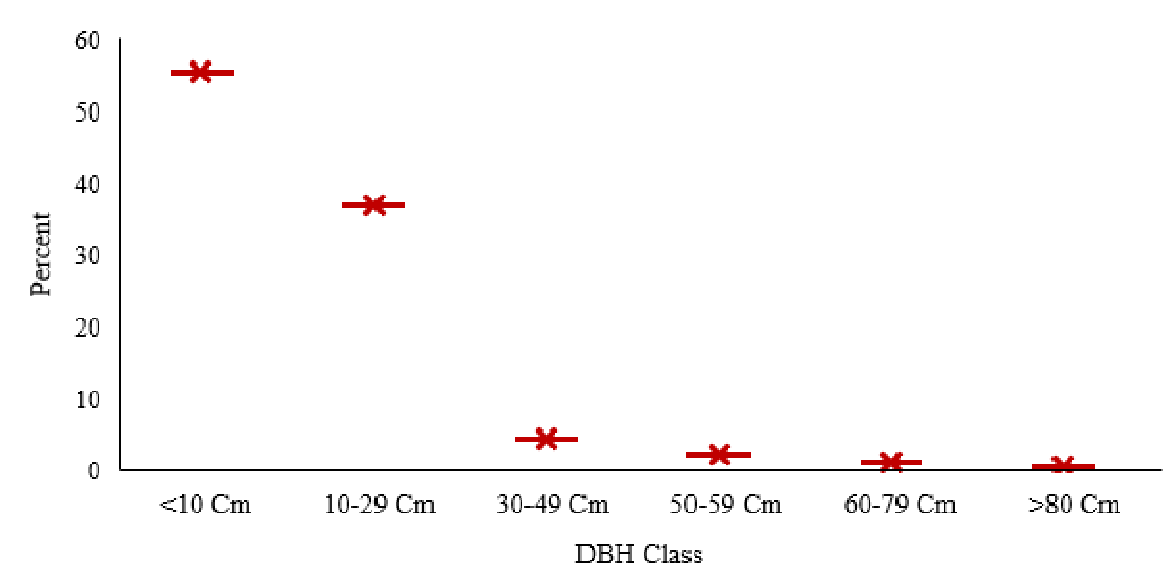


Fig. 3 Distribution of Diameter at breast height (1.3 meter).

Fig. 4 illustrated that about 52% and 36.5% of the measured height falls below 4 m and between 5-14 m respectively. Similarly, the height class from 15-24 was found to be 7.7%, and lastly, about 3.2% had DBH of above 63 m height.

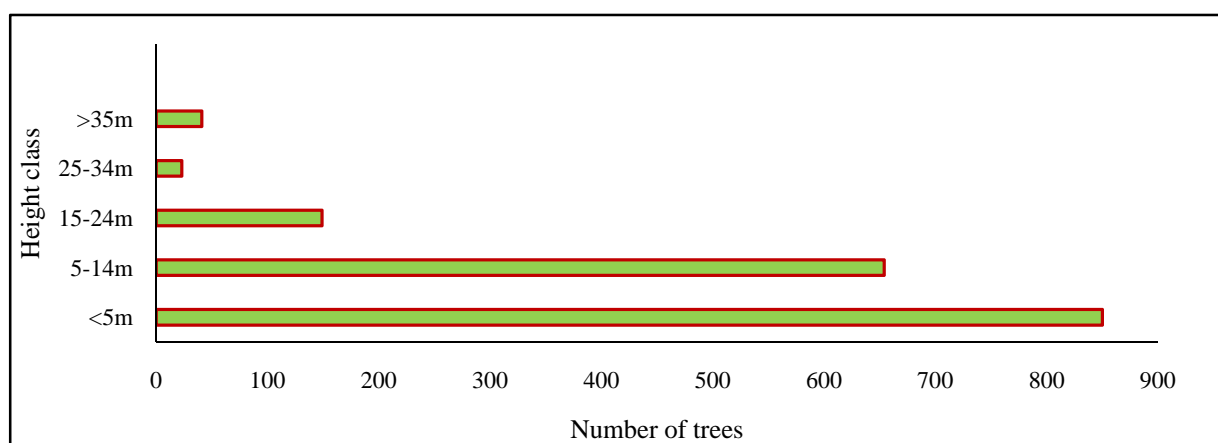


Fig. 4 Height class distribution.

3.2 Above and below-ground biomass and carbon storage

The maximum above-ground biomass and above-ground carbon of Dirmaga Watershed was found to be 1133.74 t/ha and 532.86 t/ha respectively (Table 2). Whereas the minimum above-ground biomass and above-ground carbon is 23.936 t/ha and 11.25 t/ha respectively (Table 2).

Table 2 Descriptive statistics of above and below ground carbon stock and carbon dioxide equivalent.

| | AGB(t/ha) | BGB(t/ha) | AGC(t/ha) | BGC(t/ha) | Total (AGC+BGC) | CO2 equivalent (t/ha) |
|------|-----------|-----------|-----------|-----------|-----------------|-----------------------|
| Mean | 620.14 | 124.03 | 291.47 | 24.81 | 316.27 | 1160.74 |
| Max | 1133.74 | 226.748 | 532.86 | 106.57 | 639.43 | 2346.07 |
| Min | 23.936 | 4.787 | 11.25 | 2.25 | 13.50 | 49.5 |
| SD | 365.80 | 73.16 | 171.93 | 14.63 | 186.56 | 265.80 |

The mean above-ground and below ground carbon stock in in the Woodland of Dirmaga Watershed was estimated to be 291.47 t/ha and 24.81 t/ha, respectively (Table 2). Accordingly, a mean of 1160.74 t/ha CO₂eq was sequestered in both above-ground and below ground biomass of trees and shrubs of the study area. NDVI map generated using Landsat data is shown in Fig. 2. The NDVI values ranges from 0.09 (low) to 0.35 (high) as shown in Fig. 2. The relationship between estimated forest AGC and NDVI was very strong ($r = 0.86$). The R^2 values were found to be 0.7459 and the root mean square value was 24.33 (Table 3). In general, it is possible to say that, the relationship between the vegetation indices and above ground carbon is strong.

The field-estimated AGC (above ground carbon) value ranges from 11.25 t/ha to 532.86 t/ha (Table 2) while the mean AGC is 291.47 t/ha (Table 2). The correlation ($r = 0.86$) between estimated above ground carbon and NDVI is generated using linear regression with the R^2 value of 0.7459. The mean AGC value estimated from net deference vegetation index is 271.6 t/ha. The result implies that even though, there are positive and strong relationship between field inventory based AGC and NDVI based AGC, the latter (NDVI based AGC) is underestimated.

Table 3 Relation between Above ground carbon and Landsat 8 NDVI.

| Model | Coefficient | R ² | r | RMSE | sig |
|-------------------------|-------------|----------------|------|-------|--------|
| AGC=453.46(NDVI)-58.124 | 453.46 | 0.7459 | 0.86 | 24.33 | 0.0001 |

AGC is above ground carbon, R² = Coefficient of Determination, r = regression coefficient, RMSE = root mean square error.

3.3 Trees species biomass and carbon stock contribution in the study area

The biomass carbon stock contained in each tree species in the study area was varied from one tree species to the other. tree species of *Anogeissus leiocarrpa* was found to be the first ranked contributor of biomass and carbon in the study area. Moreover, *Anogeissus leiocarrpa* (common name Kirkira) have an above ground biomass of 5953.20 t/ha and below ground biomass of 1190.64 t/ha. The result showed that tree species of *Anogeissus leiocarrpa* (common name Kirkira), *Adansonia digitata* (Diza), *Diospyros mespiliformis* (Serkin) *Tamarindus indica* L (Kumer) and *Terminalia browni* (Woyiba) had sequestered the largest portion of the total (AGC+BGC) with 3215.7 t/ha, 2657.4 t/ha, 2165.3 t/ha, 2104.5 t/ha and 1747.2 t/ha respectively. Whereas, *Ficus sycomorus* L. (Bamba), *Rhus glutinosa* (Embus), *Securinega virosa* (Roxb.) Baill. (Ashama) and *Erythrina abyssinica* (Quara) were accounted as the least biomass carbon stock reserves of 0.06 t/ha, 0.22 t/ha, 0.46 t/ha and 0.56 t/ha respectively (Table 2).

Table 4 AGB, BGB, AGC and BGC stored in each tree species of the study area.

| Species | AGB(t/ha) | BGB(t/ha) | AGC(t/ha) | BGC(t/ha) |
|---|-----------|-----------|-----------|-----------|
| <i>Acacia polyacantha</i> Willd. | 309.30 | 61.86 | 145.37 | 29.07 |
| <i>Acacia senegal</i> | 95.19 | 19.04 | 44.74 | 8.95 |
| <i>Acacia seyal</i> Del. | 740.38 | 148.08 | 347.98 | 69.60 |
| <i>Acacia sieberiana</i> Dc. | 112.82 | 22.56 | 53.03 | 10.61 |
| <i>Adansonia digitata</i> | 4920.00 | 984.00 | 2214.00 | 442.80 |
| <i>Albizia amara</i> | 37.16 | 7.43 | 17.47 | 3.49 |
| <i>Albizia malacophylla</i> (A. Rich.) | 0.99 | 0.20 | 0.47 | 0.09 |
| <i>Anogeissus leiocarrpa</i> (A. Rich.) | 5953.20 | 1190.64 | 2678.94 | 535.79 |
| <i>Balanites aegyptiaca</i> (L.) Del. | 293.89 | 58.78 | 138.13 | 27.63 |
| <i>Boscia angustifolia</i> A. Rich. | 47.35 | 9.47 | 22.26 | 4.45 |
| <i>Boswellia papyrifera</i> | 409.68 | 81.94 | 192.55 | 38.51 |
| <i>Breonadia salicina</i> | 47.48 | 9.50 | 22.31 | 4.46 |
| <i>Calotropis procera</i> | 3.59 | 0.72 | 1.69 | 0.34 |
| <i>Cobretum adenogonium</i> Steud.ex A.Rich | 456.12 | 91.22 | 214.38 | 42.88 |
| <i>Cobretum Molle</i> | 78.76 | 15.75 | 37.02 | 7.40 |
| <i>Combretum collinum</i> Fresen | 992.60 | 198.52 | 466.52 | 93.30 |
| <i>Dalbergia melanoxylon</i> Guill. & Perr | 701.29 | 140.26 | 329.61 | 65.92 |
| <i>Dichrostachys cinerea</i> | 24.63 | 4.93 | 11.57 | 2.31 |
| <i>Diospyros mespiliformis</i> | 4009.80 | 801.96 | 1804.41 | 360.88 |
| <i>Dombeya Kirikii</i> | 2.37 | 0.47 | 1.11 | 0.22 |
| <i>Erythrina abyssinica</i> | 0.99 | 0.20 | 0.47 | 0.09 |
| <i>Ficus sur</i> | 255.07 | 51.01 | 119.88 | 23.98 |
| <i>Ficus sycomorus</i> L. | 0.11 | 0.02 | 0.05 | 0.01 |

| | | | | |
|---|---------|--------|---------|--------|
| <i>Ficus thonningii</i> Blume. | 1142.35 | 228.47 | 536.91 | 107.38 |
| <i>Flueggea virosa</i> Guill. & Perr. | 11.59 | 2.32 | 5.45 | 1.09 |
| <i>Gardenia ternifolia</i> | 14.43 | 2.89 | 6.78 | 1.36 |
| <i>Giramda girar/Gemero</i> | 0.81 | 0.16 | 0.38 | 0.08 |
| <i>Grewia bicolar</i> | 7.41 | 1.48 | 3.48 | 0.70 |
| <i>Grewia mollis</i> | 44.94 | 8.99 | 21.12 | 4.22 |
| <i>Kigelia africana</i> | 1146.31 | 229.26 | 538.77 | 107.75 |
| <i>Lansea fruticosa</i> (Hochst. ex A. Rich) Engl | 514.44 | 102.89 | 241.79 | 48.36 |
| <i>Lansea welwitschii</i> | 54.17 | 10.83 | 25.46 | 5.09 |
| <i>Maytenus senegalensis</i> Forssk | 104.07 | 20.81 | 48.91 | 9.78 |
| <i>Maytenus undata</i> (Thunb.) | 1.97 | 0.39 | 0.92 | 0.18 |
| <i>Opilia campestris</i> | 2.44 | 0.49 | 1.15 | 0.23 |
| <i>Pavonia burchelli</i> | 69.12 | 13.82 | 32.49 | 6.50 |
| <i>Piliostigma thonningii</i> | 81.46 | 16.29 | 38.29 | 7.66 |
| <i>Pterocarpus lucens</i> Guill. & Perr | 748.14 | 149.63 | 351.63 | 70.33 |
| <i>Rhus glutinosa</i> | 0.39 | 0.08 | 0.18 | 0.04 |
| <i>Salix</i> Spp. | 6.85 | 1.37 | 3.22 | 0.64 |
| <i>Securidaca longepedunculata</i> | 3.99 | 0.80 | 1.88 | 0.38 |
| <i>Securinega virosa</i> (Roxb.) Baill. | 0.81 | 0.16 | 0.38 | 0.08 |
| <i>Sterculea setigera</i> Del. | 774.31 | 154.86 | 363.92 | 72.78 |
| <i>Stereospermum kunthianum</i> Cham | 84.21 | 16.84 | 39.58 | 7.92 |
| <i>Stereospermum kunthianum</i> Cham | 111.29 | 22.26 | 52.31 | 10.46 |
| <i>Tamarindus indica</i> L. | 3897.05 | 779.41 | 1753.67 | 350.73 |
| <i>Terminalia browni</i> | 3234.90 | 646.98 | 1455.71 | 291.14 |
| <i>Terminalia laxiflora</i> Engl. & Diels | 203.22 | 40.64 | 95.51 | 19.10 |
| <i>Ximenia Americana</i> L. | 2.35 | 0.47 | 1.11 | 0.22 |
| <i>Ziziphus mauritiana</i> | 11.47 | 2.29 | 5.39 | 1.08 |
| <i>Ziziphus spina-christi</i> (L.) Desf. | 241.71 | 48.34 | 113.60 | 22.72 |
| <i>Zuziphus mauritania</i> | 25.96 | 5.19 | 12.20 | 2.44 |

3.4 The total carbon stock and climate change mitigation potential of Dirmaga Watershed

The AGC and BGC of the study area were estimated to be 291.47 and 24.81 t/ha, respectively. Then which gave a total carbon stock potential of 316.27 t/ha (Table 2). The carbon pools of above-ground biomass and belowground biomass, sequestered 1069.69, and 91.05 t/ha CO₂ equivalent, respectively. This reveals that the study area has a total global climate change mitigation potential of 1160.74 t/ha CO₂ equivalents.

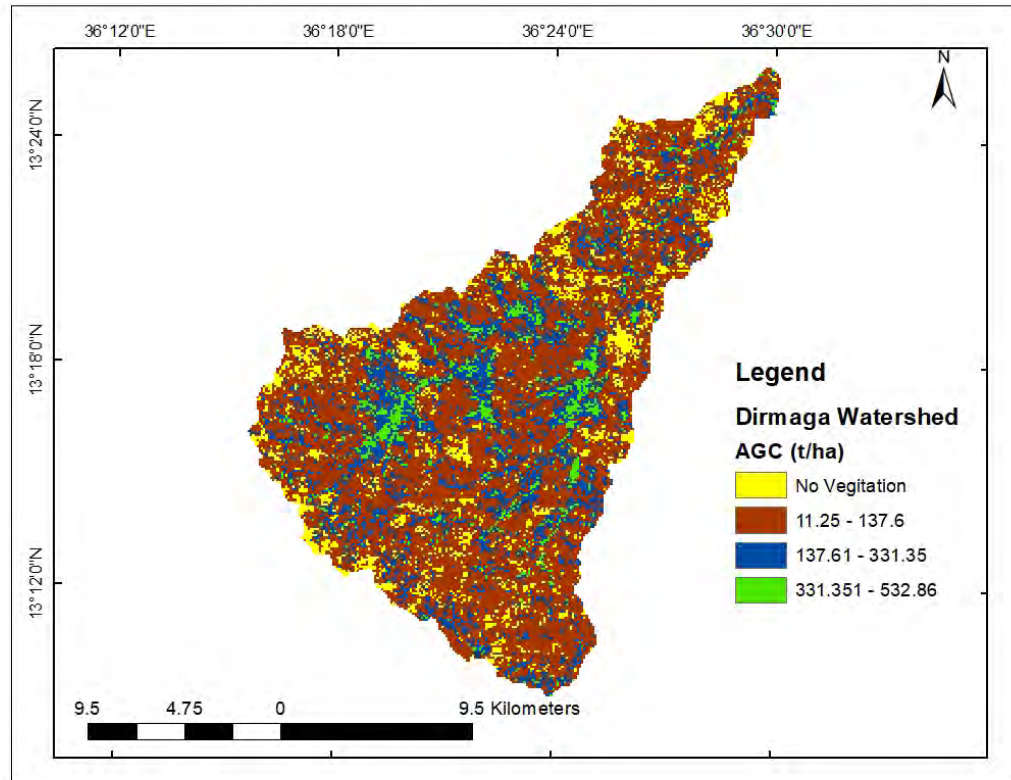


Fig. 5 The above ground carbon (t/ha) distribution of Dirmaga Watershed.

Based on NDVI estimation the spatial distribution of above ground carbon is presented in the form of map in Fig.5. From the map about 25.6% area of the watershed is non vegetated (No vegetation); where as 50.4% of the area has an above ground carbon stock value range of 11.25-137.6 t/ha; Similarly, about 19.45% and 5.55% area of the watershed was covered by above ground carbon range of 137.61-331.35 t/ha and 331.35 - 532.86 t/ha respectively (Fig. 5).

3.5 The effect of elevation and slope on the above ground carbon stock

Some study argued that, the forest biomass and carbon are highly disturbed by environmental factors like altitude (Alves et al., 2010). However, in this study the correlation between elevation (Digital elevation Model) and above ground carbon were found to be negative and very week ($r = 0.071$; $R^2 = 0.0058$) (Fig. 6).

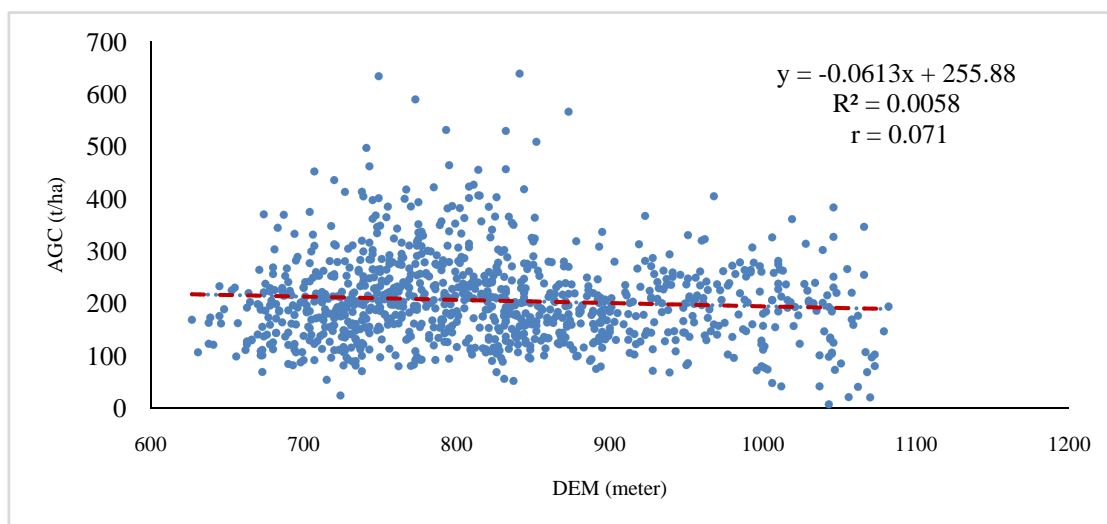


Fig. 6 The response of above ground carbon for elevation change (DEM = digital elevation model).

There is a difference in above ground carbon stock along elevation range, Even though the regression and correlation was insignificant. Mostly the mid land (750-900) was found to have relatively high amount of above ground carbon. More over the correlation between slope and above ground carbon were found to be negative and very week ($r = 0.085$; $R^2 = 0.009$) (Fig. 7).

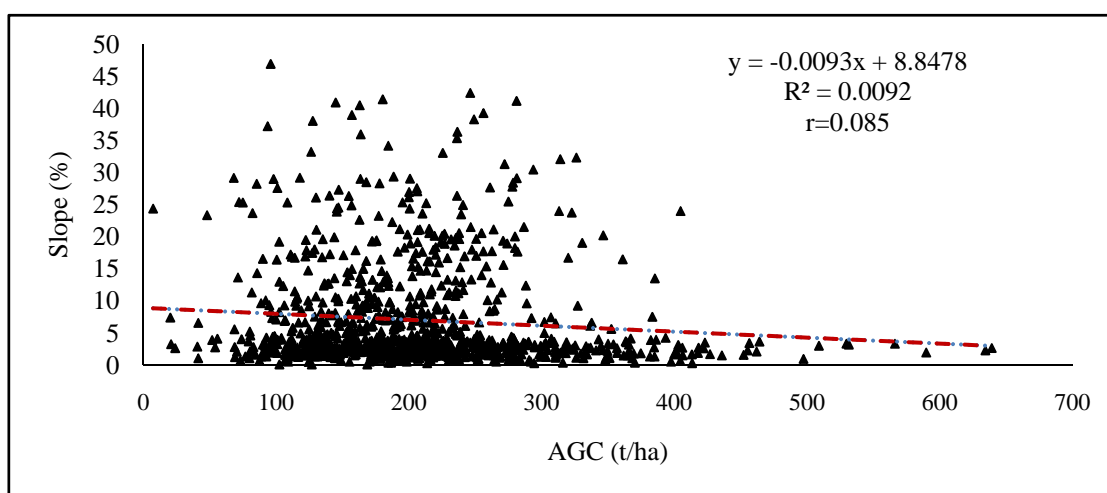


Fig.7 The effect of slope on the AGC (above ground carbon).

4 Conclusion and Recommendation

Landsat derived NDVI has a strong correlation with above ground carbon and tried to estimate and map the biomass and carbon storages in the woodland. Similarly, the mean tree species of *Anogeissus leiocarpa*, *Adansonia digitata*, *Diospyros mespiliformis*, *Tamarindus indica L.* and *Terminalia browni* sequestered the largest portion of the carbon stock. On the contrary, *Ficus sycomorus L.*, *Rhus glutinosa* and *Securinega virosa* were the least contributor of carbon stock. Generally, the woodland in the Dirmaga watershed stored above ground carbon ranged from 11.25 -532.86 t/ha based on NDVI prediction. The elevation and slope within the

watershed cannot significantly affect the biomass and carbon stock. Having observed the above result the application of vegetation indices for woodlands forest biomass and carbon estimation is appreciable but, the result is not accurate and further studies should be implemented for improvement.

Acknowledgements

The authors acknowledge with gratitude University of Gondar for fund raising and material supports. We would like to acknowledge West Armachiho District for their consistent support and assistance.

References

- Adugna F, Teshome S, Mekuria A. 2013. Forest carbon stocks and variations along altitudinal gradients in Egdu Forest: Implications of managing forests for climate change mitigation. *Science, Technology and Arts Research Journal*, 2(4)
- Alves L, Vieira S, Scaranello A, Camargo B, Santos AM, Joly A, Martinelli A. 2010. Forest Ecology and Management Forest structure and live aboveground biomass variation along an elevational gradient of tropical Atlantic moist forest (Brazil). *Forest Ecology and Management*, 260(5): 679-691
- Amsalu Abich, Asmamaw Alemu, Tadesse Mucheye, Mequanent Tebikew, Yohanns Gebremariam. 2018. Woody species diversity, productivity and carbon stock potential of dry deciduous woodland in Alitash National Park, North West Ethiopia. *International Journal of Scientific Research and Management*, 6(10): 81-98
- And SE, Hedberg I. 1995. Flora of Ethiopia And Eritrea, Canellaceae to Euphorbiaceae (Vol. 2, Part 2). Addis Ababa, Ethiopia Uppsala, Sweden: The National Herbarium, Biology Department, Science Faculty, Addis Ababa University, Ethiopia, and The Department of Systematic Botany, Uppsala University, Sweden
- Fisaha G, Hundera K, Dalle G. 2013. Woody plants' diversity, structural analysis and regeneration status of Wof Washa natural forest, North-east Ethiopia. *African Journal of Ecology*, 51(4): 599-608
- Galidaki G, Zianis D, Gitas I, Radoglou K, Karathanassi V, Tsakiri-Strati M, Woodhouse I, Mallinis, G. 2017. Vegetation biomass estimation with remote sensing: Focus on forest and other wooded land over the Mediterranean ecosystem. *International Journal of Remote Sensing*, 38: 1940-1966.
- Ib Friis SD, van B. 2010. Atlas of the potential vegetation of Ethiopia. *Atlas of the Potential Vegetation of Ethiopia*, 65(2): 321-322
- Inga H, Ensermu K, Sue Edwards SD. 2006. Flora of Etiopia and Eritrea, Gentianaceae to Cyclochelaceae (Vol 5). National Herbarium, Addis Ababa University, Addis Ababa, Ethiopia; Uppsala, Sweden
- Inga Hedberg SE. 2003. Flora Of Ethiopia And Eritrea, Apiaceae to Dipsacaceae (Vol. 4 part 1). Addis Ababa, Ethiopia; Uppsala, Sweden: The National Herbarium, Biology Department, Science Faculty, Addis Ababa University, Ethiopia and The Department of Systematic Botany Uppsala University, Sweden
- Inga Hedberg SE. 1989. Flora of ethiopia, Pittosporaceae to Araliaceae (Vol. 3). Addis Ababa and Asmara, Ethiopia Uppsala, Sweden: The National Herbarium, Biology Department, Science Faculty, Addis Ababa University, Ethiopia, and The Department of Systematic Botany, Uppsala University, Sweden
- Kent M. 2012. *Vegetation Description and Data Analysis*. The Atrium, Southern Gate, Chichester, West Sussex, John Wiley and Sons, UK
- Ketterings QM, Coe R, van Noordwijk M, Ambagau Y, Palm CA. 2001. Reducing uncertainty in the use of allometric biomass equations for predicting above-ground tree biomass in mixed secondary forests. *Forest Ecology and Management*, 146: 199-209

- Lieth H, Whittaker RH. 1975. Primary Productivity of the Biosphere (Vol 14). Springer-Verlag, Berlin, Germany
- Lu D. 2006. Review Article The potential and challenge of remote sensing-based biomass estimation. *Int. J. Remote Sens.*, 27: 1297-1328
- Lu D, Chen Q, Wang G, Liu L, Li G, Moran E. 2016. A survey of remote sensing-based aboveground biomass estimation methods in forest ecosystems. *International Journal of Digital Earth*, 9: 63–105.
- Mitchard ETA, Saatchi SS, Woodhouse IH, Nangendo G, Ribeiro NS, et al. 2009. Using satellite radar backscatter to predict above-ground woody biomass: A consistent relationship across four different African landscapes. *Geophysical Research Letters*, 36
- Petit J, Jouzel J, Raynaud D, Barkov NI, Barnola JM, Basile I, Bender M, Chappelaz J, Davis M, Delaygue G, Delmote M. 1999. Climate and atmospheric history of the past 420,000 years from the Vostok ice core in Antarctica. *Nature*, 339: 429-436
- Rani M, Kumar P, Pandey PC, Srivastava PK, Chaudhary B, Tomar V, Mandal VP. 2018. Multi-temporal NDVI and surface temperature analysis for Urban Heat Island inbuilt surrounding of sub-humid region: a case study of two geographical regions. *Remote Sensing Applications: Society and Environment*, 10: 163-172
- Safari A, Sohrabi H, Powell S, Shataee S. 2017. A comparative assessment of multi-temporal Landsat 8 and machine learning algorithms for estimating aboveground carbon stock in coppice oak forests. *International Journal of Remote Sensing*, 38: 6407-6432
- Senbeta F, Teketay D. 2001. Regeneration of indigenous woody species under the canopies of tree plantations in Central Ethiopia. *Tropical Ecology*, 42(2): 175-185
- Sue Edwards, Sebsebe Demissew IH. 1997. *Flora of Ethiopia and Eritrea (Vol. 6)*. Addis Ababa, Ethiopia: The National Herbarium, Biology Department, Science Faculty, Addis Ababa University, Ethiopia, and The Department of Systematic Botany, Uppsala University, Sweden
- Sun G, Ranson KJ, Guo Z, Zhang Z, Montesano P, Kimes D. 2011. Forest biomass mapping from lidar and radar synergies. *Remote Sensing of Environment*, 115: 2906-2916
- Sun H, Qie G, Wang G, Tan Y, Li J, Peng Y, Ma Z, Luo, C. 2015. Increasing the accuracy of mapping urban forest carbon density by combining spatial modeling and spectral unmixing analysis. *Remote Sensing*, 7: 15114-15139
- Temesgen F. 2020. *Woody Species Structure and Regeneration Status in Kafta Sheraro National Park Dry Forest, Tigray Region, Ethiopia*. doi: 10.20944/preprints202002.0446.v1
- Tian X, Li Z, Su Z, Chen E, et al. 2014. Estimating montane forest above-ground biomass in the upper reaches of the Heihe River Basin using Landsat-TM data. *International Journal of Remote Sensing*, 35: 7339-7362
- Tucker CJ. 1979. Red and photographic infrared linear combinations for monitoring vegetation. *Remote Sensing of Environment*, 8(2): 127-150
- West PW. 2009. *Tree and Forest Measurement (2nd ed)*. Springer: Berlin, Germany
- Zhu X, Liu D. 2015. Improving forest aboveground biomass estimation using seasonal Landsat NDVI time-series. *ISPRS Journal of Photogrammetry and Remote Sensing*, 2015
- Zhu C, Lu D, Victoria D, Dutra LV. 2016. Mapping fractional cropland distribution in Mato Grosso, Brazil using time series MODIS enhanced vegetation index and Landsat Thematic Mapper data. *Remote Sensing*, 8: 22